

Single Oligomer Spectra Probe Chromophore Nanoenvironments of Tetrameric Fluorescent Proteins

Christian Blum,[†] Alfred J. Meixner,[‡] and Vinod Subramaniam*[†]

Contribution from the Biophysical Engineering Group, MESA+ Institute for Nanotechnology and Institute for Biomedical Technology, Faculty of Science and Technology, University of Twente, P.O. Box 217, 7500 AE Enschede, The Netherlands, and Institut für Physikalische und Theoretische Chemie, University of Tuebingen, Auf der Morgenstelle 8, 72076 Tübingen, Germany

Received January 31, 2006; E-mail: c.blum@utwente.nl; v.subramaniam@utwente.nl

Abstract: When analyzing the emission of a large number of individual chromophores embedded in a matrix, the spread of the observed parameters is a characteristic property for the particular chromophore–matrix system. To quantitatively assess the influence of the matrix on the single molecule emission parameters, it is imperative to have a system with a well-defined chromophore nanoenvironment and the possibility to alter these surroundings in a precisely controlled way. Such a system is available in the form of the visible fluorescent proteins, where the chromophore nanoenvironment is defined by the specific protein sequence. We analyze the influence of the chromophore embedding within this defined protein environment on the distribution of the emission maximum wavelength for a number of variants of the fluorescent protein DsRed, and show that this parameter is characteristic of the chromophore–protein matrix combination and largely independent of experimental conditions. We observe that the chemical changes in the vicinity of the chromophore of different variants do not account for the different distributions of emission maximum positions but that the flexibility of the chromophore surrounding has a dominant role in determining the distribution. We find, surprisingly, that the more rigid the chromophore surrounding, the broader the distribution of observed maximum positions. We hypothesize that, after a thermally induced reorientation in the chromophore surrounding, a more flexible system can easily return to its energetic minimum position by fast reorientation, while in more rigid systems the return to the energetic minimum occurs in a stepwise fashion, leading to the broader distribution observed.

Introduction

In contrast to classical bulk spectroscopy, single molecule spectroscopy yields detailed insights into the spatial and temporal heterogeneity of single emitters. The heterogeneity of spectral properties of single molecules is due to the fact that any nongas-phase chromophore interacts with its immediate environment; this specific chromophore–environment system determines the exact photophysical properties of the emitter. Local variations in the nanoenvironment of a single chromophore lead to spatial and temporal heterogeneity of the spectral properties of the chromophore. The heterogeneity of single molecule spectral parameters has been shown for single emitters at cryogenic temperatures and at room temperature. These studies have demonstrated a distribution of various photophysical parameters, such as fluorescent lifetime and intensity and the emission maximum positions of individual spectra.^{1–3} In some cases, the observed changes could be attributed to intrinsic properties such as conformational changes

in the emitting chromophore,⁴ but in most cases the observed heterogeneity was attributed to extrinsic factors such as varying matrix–chromophore interactions.^{3,5,6} Especially at room temperature little is known about the predominant interactions influencing spectral parameters of an embedded chromophore. The observed spectral heterogeneity has been qualitatively explained by rearrangements in the host matrix around the emitter, and indeed the spread of the parameters observed upon analysis of the emission of a large number of embedded individual chromophores is a characteristic of the particular chromophore–matrix system. In this manner, single molecule spectroscopy has been used recently to characterize polymer properties using single dye molecules sensitive to local density fluctuations.^{2,7}

In general, we envision two mechanisms that could possibly dominate the spread of spectral parameters. In the first case, interactions between the chromophore and specific atom groups

[†] University of Twente.

[‡] University of Tuebingen.

- (1) Weston, K. D.; Buratto, S. K. *J. Phys. Chem. A* **1998**, *102*, 3635–3638.
- (2) Vallee, R. A. L.; Tomczak, N.; Vancso, G. J.; Kuipers, L.; van Hulst, N. *F. J. Chem. Phys.* **2005**, *122*.
- (3) Wang, H. M.; Bardo, A. M.; Collinson, M. M.; Higgins, D. A. *J. Phys. Chem. B* **1998**, *102*, 7231–7237.

(4) Stracke, F.; Blum, C.; Becker, S.; Müllen, K.; Meixner, A. *Chem. Phys. Lett.* **2000**, *325*, 196–202.

(5) Vallee, R. A. L.; Vancso, G. J.; van Hulst, N. F.; Calbert, J. P.; Cornil, J.; Bredas, J. L. *Chem. Phys. Lett.* **2003**, *372*, 282–287.

(6) Stracke, F.; Blum, C.; Becker, S.; Müllen, K.; Meixner, A. *J. Chem. Phys.* **2004**, *300*, 153–164.

(7) Vallee, R. A. L.; Marsal, P.; Braeken, E.; Habuchi, S.; De Schryver, F. C.; Van der Auweraer, M.; Beljonne, D.; Hofkens, J. *J. Am. Chem. Soc.* **2005**, *127*, 12011–12020.

of the surrounding matrix influence the spectral distributions. In this situation certain atoms or atom groups of the matrix affect the emission more strongly than others when interacting with the embedded chromophore. Thus, varying the chemical composition of the matrix can reveal the influence of these interactions on the distribution of spectral parameters. In the second case, unspecific interactions related to the flexibility of the chromophore environment may play a key role. In a flexible environment a multitude of interactions are possible, which can lead to a broader distribution of the observed parameters if these interactions are stable long enough to detect them. On the other hand a flexible environment can lead to a more narrow spectral distribution if the system is able to very rapidly relax to energetically favorable conformations.

To quantitatively analyze the effect on the distribution of spectral parameters of the embedding of a chromophore into its surrounding, the chromophore–polymer systems are not ideal. In these systems the polymer chains form a random environment around the chromophore so that the exact details of the chromophore nanoenvironment are not known. Furthermore the influence of irregularities and impurities in the polymer matrix are difficult to account for. Thus, a system with a well-defined chromophore surrounding and the possibility to alter these surroundings in a precisely controlled way is needed. Such a system is conveniently available in the form of the visible fluorescent proteins (VFPs). In contrast to the largely random surrounding of chromophores embedded in polymer films, in fluorescent proteins the immediate nanoenvironment of the chromophore is well-defined by the rest of the protein. VFPs share a distinctive tertiary structure, where the protein backbone forms a beta-barrel cylinder defined by beta sheets within which the VFP chromophore, which is formed by an autocatalytic reaction, is located.^{8,9} The chromophore is thus completely surrounded by the protein and has no direct contact with the solvent environment. In VFPs the beta sheets of the protein encapsulating the chromophore constitute the embedding matrix. Site-directed mutagenesis in and around the chromophore has yielded a wide range of mutant VFPs, such that a whole palette of proteins with different chromophore environments, and thus well-defined chromophore–matrix systems, are available.^{10,11}

The definition of such a chromophore environment is however not sufficient to ensure fixed spectral characteristics of the VFPs, and distributions of spectral parameters of VFPs have been demonstrated at the single molecule level.¹² Individual protein molecules display structural heterogeneity on different time scales. Thus even for chemically well-defined protein nanoenvironments, the observed spectral heterogeneity must reflect a structural variation of the chromophore nanoenvironment leading to a multitude of different chromophore–matrix interactions. To analyze in detail the influence of the chromophore embedding on the distribution of the emission maximum position we chose a number of variants derived from the *Discosoma* red fluorescent protein, DsRed. Fluorescent proteins from the DsRed family can form green and red emitting

chromophores,^{13,14} so that, for certain variants, the emission from two spectrally distinct chromophores embedded in essentially the same surroundings can be analyzed.

The development of fluorescence in DsRed involves a maturation process leading from a nonfluorescent state to the final red fluorescent protein via a green fluorescent intermediate¹⁵ which has recently been proposed to be a dead end side product.¹⁶ The green fluorescence is thought to arise from a chromophore similar to that found in the *Aequoria* green fluorescent protein, an assumption that has been verified by a recent crystal structure of DsRed with mature and immature chromophores.¹⁷ The mechanism of the chromophore formation remains a matter of debate, with a recent proposal by Lukyanov and co-workers suggesting a scheme for the chromophore formation in which a GFP-like protonated (neutral) state is the branching point between the formation of the green-emitting chromophore and the red-emitting, mature, chromophore.¹⁶ This implies that within one protein a red- or a green-emitting chromophore can be formed. Recent X-ray studies showed differences in the nanoenvironments of the GFP-like and mature chromophore in DsRed, attributed to the chemical reactions resulting in the different chromophores and to the different steric demands of the chromophores,¹⁷ while leaving unchanged the principal structure of the scaffold surrounding the GFP-like and mature chromophores.

We were especially interested in whether the different chemical surroundings and packing of the chromophores within the different protein variants affect the distribution of photophysical parameters observable at the single molecule level. We used spectrally resolved single molecule emission spectroscopy to sample the evolution of the single oligomer emission. The emission spectra of single molecules are very sensitive to heterogeneous chromophore–matrix interactions, yielding fluctuations of different observable parameters.¹⁸ Here we have generated histograms of the single oligomer emission maximum positions and analyzed the resulting distributions. This parameter has been proven to be highly sensitive to changes in the chromophore surrounding, and fluctuations in this observable reveal, among other effects, excursions of the molecule into distinct photophysical states (“spectral jumps”) or subtle effects of the environment on the spectrum leading to “spectral diffusion”.^{18,19}

We have focused our analyses on a range of DsRed variants that have recently become available. Amino acid substitutions in these variants yield proteins with altered spectral and maturation properties.²⁰ These substitutions, when situated in the vicinity of the chromophore, also have an effect on the flexibility of the chromophore surrounding and on the chemical nanoenvironment of the chromophore.

There is limited structural data on DsRed variants. Crystal structures of DsRed and very few mutants expressing the mature

(8) Yang, F.; Moss, L.; Phillips, G. *Nat. Biotechnol.* **1996**, *14*.

(9) Ormö, M.; Cubitt, A.; Kallio, K.; Gross, L.; Tsien, R.; Remington, S. *Science* **1996**, *272*, 1392–1395.

(10) Tsien, R. A. *Rev. Biochem.* **1998**, *67*, 509.

(11) Shaner, N. C.; Campbell, R. E.; Steinbach, P. A.; Giepmans, B. N. G.; Palmer, A. E.; Tsien, R. Y. *Nat. Biotechnol.* **2004**, *22*, 1567–1572.

(12) Blum, C.; Meixner, A. J.; Subramaniam, V. *Biophys. J.* **2004**, *87*, 4172–4179.

(13) Yarbrough, D.; Wachter, R.; Kallio, K.; Matz, M.; Remington, S. *PNAS* **2001**, *98*, 462–467.

(14) Wall, M.; Socolich, M.; Ranganathan, R. *Nat. Struct. Biol.* **2000**, *7*, 1089.

(15) Gross, L.; Baird, G.; Hoffman, R.; Baldrige, K.; Tsien, R. *PNAS* **2000**, *97*, 11990–11995.

(16) Verkhusha, V. V.; Chudakov, D. M.; Gurskaya, N. G.; Lukyanov, S.; Lukyanov, K. A. *Chem. Biol.* **2004**, *11*, 845–854.

(17) Tubbs, J. L.; Tainer, J. A.; Getzoff, E. D. *Biochemistry* **2005**, *44*, 9833–9840.

(18) Blum, C.; Stracke, F.; Becker, S.; Müllen, K.; Meixner, A. *J. Phys. Chem. A* **2001**, *105*, 6983–6990.

(19) Stracke, F.; Blum, C.; Becker, S.; Müllen, K.; Meixner, A. *J. ChemPhysChem* **2005**, *6*, 1242–1246.

(20) Bevis, B. J.; Glick, B. S. *Nat. Biotechnol.* **2002**, *20*, 83–87.

and immature chromophore are available.^{13,14,17} Based on these data, it is possible to reason which amino acid substitutions have the potential to change the chemical environment of the chromophore. Although the crystal structures of the DsRed variants studied here are still unknown, protein modeling data are available that describe the influence of the packing of the chromophore on the maturation speed and the final green to red emission ratio of the proteins²¹ which makes it possible to qualitatively compare the different flexibilities of the chromophore environment of distinct variants.

Here we aim to compare the distribution of single oligomer emission maximum positions for different variants of proteins from the DsRed group. This distribution is determined by room temperature spectrally resolved single molecule emission spectroscopy measurements on a large number of single tetramers. We find a clear correlation between the distribution width and the nominal flexibility of the chromophore surrounding.

Materials and Methods

The coding sequence of DsRed from the pDsRed-N1 expression vector (BD Biosciences Clontech, Palo Alto, CA) was inserted into the pRSETa vector (Invitrogen, Carlsbad, CA), thereby adding six histidines to its amino terminus (6His-tag). The expression of 6His-tagged DsRed in *E. coli* BL21(DE3) cells was induced by 1 mM IPTG for various lengths of time (3–24 h). To purify DsRed-6His the clarified cell lysate was adsorbed on Nickel-NTA agarose (Qiagen, Hilden, Germany) overnight at 4 °C, and DsRed-6His was eluted with 250 mM imidazole. The eluted fractions were dialyzed against 100 mM Tris-HCl, pH 8.5, 100 mM NaCl overnight.

In addition to DsRed, we have examined the photophysical properties of the following variants: DsRed2 (Arg2Ala, Lys5Glu, Lys9Thr, Val105Ala, Ile161Thr, Ser197Ala), Fluorescent Timer (Val105Ala, Ser197Thr), DsRed_N42H (Asn42His), and AG4 (Val71Met, Val105Ala, Ser197Thr).

The DsRed2, Fluorescent Timer, DsRed_N42H, and AG4 mutants were produced by standard site-directed mutagenesis approaches as reported previously.²² The PCR products were cloned into a pQE-30/BamHI/Hind III vector. *Escherichia coli* JM101 cells were transformed with the plasmids and were grown as above. Protein purification proceeded as described above.

The single molecule studies were performed with a scanning stage confocal fluorescence microscopy set up for optical single molecule detection and spectroscopy (for details see ref 18). A single line argon-ion laser served as the light source for excitation at 458 and 488 nm. The excitation intensity was stabilized by a feedback control loop and was on the order of 2 kW/cm² and 5 kW/cm², respectively, well below the fluorescence saturation intensity of DsRed.²³ The collected fluorescence light was separated from scattered excitation light by an appropriate holographic notch filter (Kaiser Optical Systems Inc., Ann Arbor, Michigan).

Sample preparation of the VFPs was accomplished by preparing a dilution series in 100 mM Na cacodylate buffer, pH 7.5. The diluted solution was finally mixed with a solution of 2 g Poly(vinyl alcohol) ("PVA", Mowiol 40–88, Hoechst, Frankfurt Main, Germany) in 100 mL of cacodylate buffer. The VFP/PVA solution was then spin-coated onto a microscopy cover slide.

Great care was taken to ensure that the prepared samples were free of fluorescing contaminations. The buffer and PVA solutions were first

irradiated with intense white light and subsequently with 5 W of laser light from an argon-ion laser operating in "all lines" mode to bleach any fluorescing contaminants in the solutions. Sample preparation was carried out under a cleanroom laminar flow bench. The microscopy cover slides used as substrate were kept under chromosulfuric acid and rinsed first with triple distilled water immediately prior to sample preparation and then with methanol (Merck, Uvasol, Darmstadt, Germany) before drying.

The absence of fluorescing impurities in the buffer, the PVA, and the cover slides was verified by preparing negative control samples of buffer and PVA matrix alone on cover slides treated as above.

All single molecule experiments were carried out at room temperature (~22 °C) and at ambient conditions. Fluorescence intensity images were obtained by raster scanning the sample and detecting the emission intensity with an avalanche photodiode (SPCM 200, EG&G, Gaithersburg, MD). From these images distinct diffraction limited fluorescence spots were selected for spectrally resolved investigations. Fluorescence spectra were acquired by a spectrometer (SpectraPro 300i, Acton Research Corporation, Acton, MA) and a liquid nitrogen cooled CCD camera (LN/CCD-100PB, Princeton Instruments, Trenton, NJ). We recorded spectral sequences as rapid successions of single molecule fluorescence spectra with an integration time of 1 s each, with less than a 25 ms dead time lag between each spectrum. The spectrometer was wavelength calibrated based on the use of laser lines, and a background spectrum, recorded in the absence of sample but with all other conditions being the same, was subtracted from each spectrum.

To determine the maximum intensity and peak position of each fluorescence spectrum systematically and with high accuracy, a double Gaussian curve was fitted to each raw single molecule spectrum (see Figure 2). A double Gaussian curve is the minimum required for a good fit to the simple vibronic progression of the VFP emission spectra, while more components overfit the spectra.

Bulk fluorescence spectra of DsRed variants were collected on a Varian Cary Eclipse fluorescence spectrophotometer. Spectra were corrected using fluorescence standards.

The consistency between the emission maximum positions of the GFP-like and the mature chromophore on the two spectrometers used was checked by comparing bulk spectra recorded on both spectrometers and was found to agree better than 1.5 nm.

Results and Discussion

We analyzed the emission of the fluorescent protein DsRed and its variants DsRed2, Fluorescent Timer, DsRed_N42H, and AG4 (for ensemble spectra see Figure 1). All of the proteins studied here form obligate tetramers even at the nanomolar concentrations used for single molecule experiments. Thus, in our experimental situation, we expect to mainly sample tetramers. In tetramers containing both GFP-like green-emitting and mature red-emitting chromophores, a coupling of these chromophores by fluorescence resonance energy transfer (FRET) is a theoretical possibility. However, single tetramers that exhibit all green or all red fluorescence show no difference to the behavior of tetramers yielding mixed emission, indicating that FRET is not a complicating factor in this experiment. In general we expect that single oligomer spectra will include contributions from one or both chromophore species.

We analyzed the emission from a large number of molecules from each of the five variants studied (see Table 1). To identify the distribution of the spectral positions of a single protein oligomer, we determined the fluorescence maximum position of the respective emission band by fitting a double Gaussian (for examples of typical single entity spectra and fitted double Gaussians, see Figure 2) and then generated separate histograms

(21) Terskikh, A.; Fradkov, A. A. Z.; Kajava, A.; Angres, B. *J. Biol. Chem.* **2002**, *277*, 7633–7636.

(22) Terskikh, A.; Fradkov, A.; Ermakova, G.; Zaraisky, A.; Tan, P.; Kajava, A.; Zhao, X.; Lukyanov, S.; Matz, M.; Kim, S.; Weissman, I.; Siebert, P. *Science* **2000**, *290*, 1585–1588.

(23) Harms, G.; Cognet, L.; Lommerse, P.; Blab, G.; Schmidt, T. *Biophys. J.* **2001**, *80*, 2396–2408.

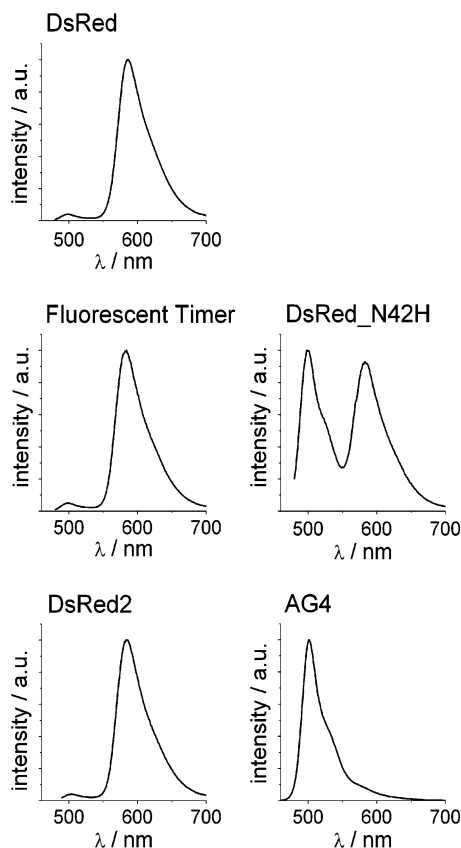


Figure 1. Ensemble emission spectra of DsRed and the analyzed variants. The emission of DsRed and the variants DsRed2 and Fluorescent Timer is dominated by the emission from the matured chromophore with peak ~ 583 nm, whereas some emission from the GFP-like green-emitting chromophore can be detected around 500 nm. Though the emission spectra are very similar, DsRed2 and Fluorescent Timer show a different maturation speed of the red-emitting chromophore than DsRed. DsRed_N42H shows two strong emission bands originating from the GFP-like as well as the matured chromophore; the emission of the variant AG4 is dominated by the emission from the GFP-like chromophore with emission maximum ~ 500 nm.

Table 1

variant	single oligomer spectroscopy			maximum position distribution width, nm
	excitation wavelength, nm	number of sampled units	number of acquired spectra	
DsRed	488	539	2263	7.4 ^a
Fluorescent Timer	488	258	894	8.3 ^a
DsRed2	488	129	420	5.0 ^a
AG4	458	276	689	10.0 ^b
DsRed_N42H	458	315	1379	7.0 ^b and 9.0 ^a

^a Red-emitting, mature chromophore. ^b Green-emitting, GFP-like chromophore.

for the emission maximum position of each spectrum collected from each of the different variants. In our analysis, we focused on the dominating spectral form or forms of each variant and excluded minor subensembles such as the weak green emission of DsRed.

Corresponding to the bulk spectra, DsRed, DsRed2, Fluorescent Timer, and AG4 showed one main distribution from the respective dominant chromophore emission (see Figure 3a, b, c, f), whereas DsRed_N42H shows two significant distributions, one originating from the emission of the GFP-like

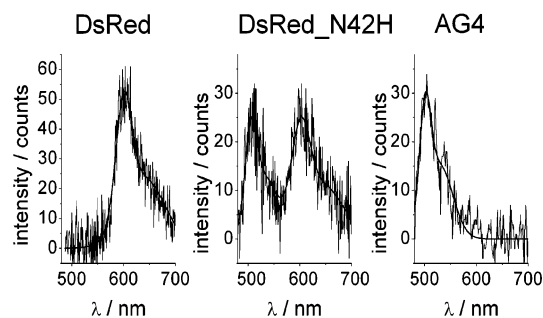


Figure 2. Typical single oligomer emission spectra of proteins from the DsRed group. The single oligomer spectra from DsRed, as well as its variants Fluorescent Timer and DsRed2, showed predominantly red emission from the matured chromophore, the spectra from the variant AG4, mainly green emission from the GFP-like chromophore, and the spectra from the variant DsRed_N42H, mainly mixed emission from both different chromophores. To determine the maximum emission wavelength of the spectra we fitted a double Gaussian to each emission band.

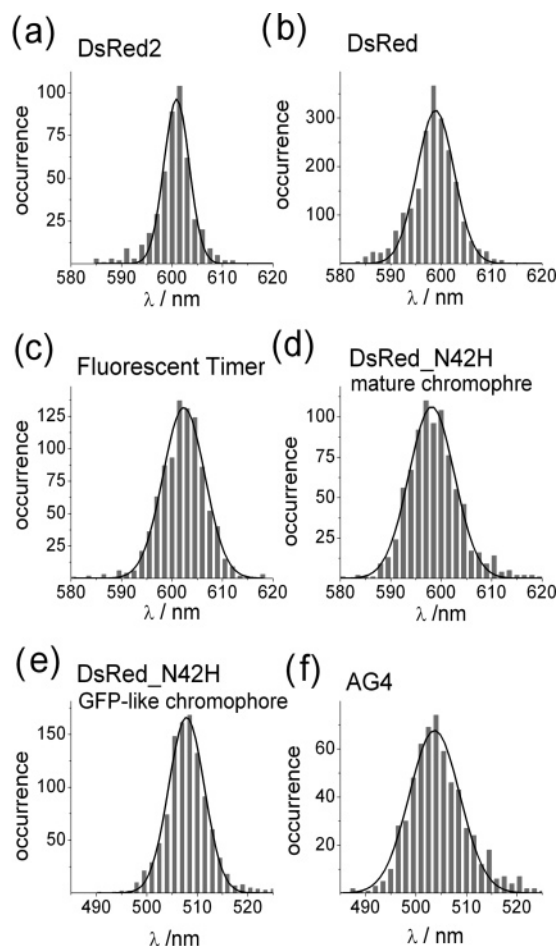


Figure 3. Distribution of single oligomer emission maximum positions. We assembled the emission maximum positions of the predominant forms into histograms. To determine the width of the distribution we fitted a Gaussian to the distribution. The width of the distribution is clearly characteristic for each variant. Parts a–d show the distribution of maximum positions from matured chromophores; parts e and f show the distribution of maximum positions from GFP-like chromophores.

chromophore and the other which can be attributed to the mature chromophore (see Figure 3d, e).

The histograms of the emission maximum positions of AG4 and DsRed_N42H confirm that the spectral position of the GFP-like chromophores is distributed around the maximum position of the bulk emission. We find clear Gaussian distributions for

the GFP-like chromophores of AG4 and DsRed_N42H centered at 503 nm and 507 nm (Figure 3e, f).

Contrary to the emission of the GFP-like chromophore the observed single entity emission of the mature chromophore is in almost all cases notably red shifted compared to bulk samples. The histogram of the observed maximum positions of all spectra (Figure 3a–d) confirms the general red shift of the mature chromophore emission away from the bulk emission maximum at 583 nm. The distribution of the red emission shows a clear Gaussian shape with mean positions of 599 nm for DsRed, 598 nm for DsRed_N42H, 601 nm for DsRed2, and 602 nm for Fluorescent Timer. We attribute this red shift to a rapid, photoinduced formation of the super red form of the mature chromophore. This super red form has been detected by different means,^{24–26} but its exclusive detection under single molecule detection conditions has not yet been reported. Under the experimental conditions employed in this study, we exclusively find the super-red form for all sampled DsRed variants. The nature of the super-red form has been elucidated by Habuchi et al.²⁷ and has also been observed in high-resolution hole-burning experiments.²⁵ The super-red form observed here has identical origins for all sampled variants and can thus be directly compared in our analysis.

Although the mean positions of the distributions of the emission maxima of the respective chromophores are comparable, the standard deviations of the distributions clearly show differences between the various DsRed variants.

The distribution of photophysical parameters is determined by the chromophore itself and by extrinsic factors determined by the chromophore interaction with its immediate nanoenvironment.¹⁹ Thus one would expect that different chromophores embedded in the same environment result in different distributions of the observable. This dependence of the single oligomer emission maximum distribution on the specific chromophore can clearly be seen with the variant DsRed_N42H. DsRed_N42H shows distinct emission of both the GFP-like and the mature chromophore which made it possible to analyze the emission distribution of these chromophores under identical experimental parameters and chromophore environments. In Figure 3d and e we present the distributions of the maximum positions for DsRed_N42H and find a standard deviation of $2\sigma = 7.0$ nm for the GFP-like chromophore and a markedly different standard deviation of $2\sigma = 9.0$ nm for the mature chromophore.

On the other hand the distribution of fluorescence maximum positions of a chromophore in one spectral form is also influenced by extrinsic variations such as differences between individual proteins caused by slightly varied chromophore surroundings and by variations of the chromophore surrounding with time, an effect often referred to as “spectral diffusion”.

If the maximum position distribution of one specific chromophore is indeed determined by chromophore–matrix interactions and is not influenced by the experiment, e.g., photoinduced, then the distribution is largely independent of the applied

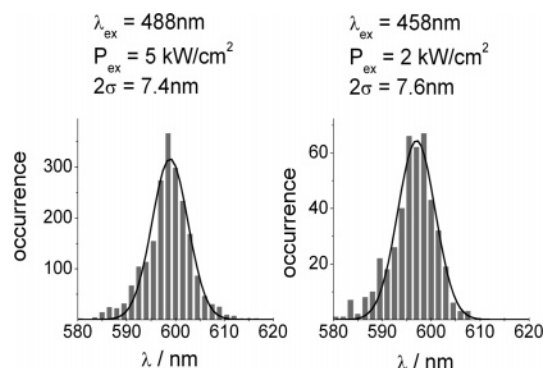


Figure 4. Distribution of emission maximum positions of DsRed using different excitation wavelength and excitation powers. The change of the excitation wavelength and the excitation power does not change the width of the distribution ($2\sigma = 7.4$ nm and $2\sigma = 7.6$ nm); hence the width of the distribution is independent of these parameters.

experimental conditions such as excitation power and excitation wavelength. To verify if the standard deviation of emission maximum positions is indeed independent of excitation power and excitation wavelength, we excited single oligomers of DsRed with 458 nm at 2 kW/cm². After assembling the determined emission maximum positions into a histogram in the same manner as that for excitation with 488 nm at 5 kW/cm², we found the standard deviation of the emission maximum of DsRed excited at 458 nm to be $2\sigma = 7.6$ nm which is in very good agreement with the value $2\sigma = 7.4$ nm determined for exciting DsRed at 488 nm (see Figure 4).

As the different variants of fluorescent proteins we analyzed here all have slight alterations of the protein structure in the chromophore surrounding, we expect the width of the emission maximum distribution to be a characteristic of each variant. Analyzing the emission of the super-red form of the mature chromophore, we find that DsRed2 shows the most narrow distribution with $2\sigma = 5.0$ nm, followed by DsRed with $2\sigma = 7.4$ nm, Fluorescent Timer with $2\sigma = 8.3$ nm, and DsRed_N42H with $2\sigma = 9.0$ nm. When looking at the GFP-like chromophore we find $2\sigma = 7.0$ nm for DsRed_N42H and $2\sigma = 10.0$ nm for AG4 (see Figure 3). Evidently the small changes in the chromophore environment introduced by the mutation of DsRed do not cause distinct changes in bulk emission maximum positions but do cause significant differences in the standard deviation of the single oligomer emission maximum positions.

Since the heterogeneity of spectral parameters observed in single molecule experiments is due to rearrangements in the host matrix around the emitter, the observed differences in the distribution of the single molecule emission maximum position point toward changes in the rigidity of the chromophore nanoenvironment in the different variants analyzed. This agrees with a model of Terskikh et al. who showed that different DsRed variants exhibit differences in the flexibility of the chromophore nanoenvironment which results in different maturation speeds and the final ratio of green to red emission of the protein samples.²¹ Since there are very limited data on structures of DsRed variants available, these authors used protein modeling techniques based on the known DsRed structure, to validate the chromophore nanoenvironment. They argued that bulky amino acid residues close to the chromophore restrict the necessary movement of the maturing chromophore and thereby lead to slow and less complete maturing variants. On the other hand substituting amino acids in the vicinity of the chromophore by

(24) Malvezzi-Campeggi, F.; Jahnz, M.; Heinze, K.; Dittrich, P.; Schwille, P. *Biophys. J.* **2001**, *81*, 1776–1785.

(25) Bonsma, S.; Gallus, J.; Konz, F.; Purchase, R.; Volker, S. *J. Lumin.* **2004**, *107*, 203–212.

(26) Cotlet, M.; Hofkens, J.; Habuchi, S.; Dirix, G.; Van Guyse, M.; Michiels, J.; Vanderleyden, J.; De Schryver, F. *PNAS* **2001**, *98*, 14398–14403.

(27) Habuchi, S.; Cotlet, M.; Gensch, T.; Bednarz, T.; Haber-Pohlmeier, S.; Rozenski, J.; Dirix, G.; Michiels, J.; Vanderleyden, J.; Heberle, J.; De Schryver, F. C.; Hofkens, J. *J. Am. Chem. Soc.* **2005**, *127*, 8977–8984.

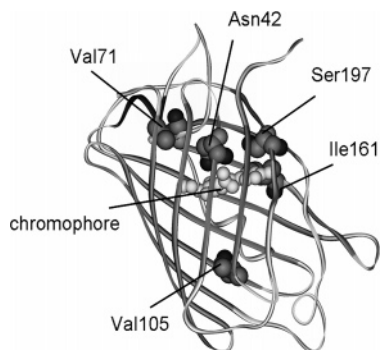


Figure 5. Ribbon scheme of the three-dimensional structure of DsRed;¹⁴ the chromophore and the residues which were changed in the chromophore environment of the variants we used are in space-filling presentation. These changes have direct influence on the distribution of the single oligomer emission maximum position. The dominating factor influencing this distribution is the change in the flexibility of the chromophore environment, while the chemical changes in the chromophores nanoenvironment play only a secondary role in the fluorescent proteins analyzed here.

amino acids with smaller residues increases the flexibility around the forming chromophore and thereby accelerates maturation and leads to a smaller ratio of GFP-like to mature chromophores. Using the concept of Terskikh et al. the relative rigidity of the embedding of the chromophore can be judged by looking at the maturation speed and the final ratio of green to red emission of the protein samples.

In DsRed2 the substitutions Val-105-Ala, Ile-161-Thr, and Ser-197-Ala in the vicinity of the chromophore all substitute a larger residue for a smaller one. The amino acids 161 and 197 are in the immediate vicinity of the chromophore, and their substitution is thus likely to directly influence the chromophore environment. Val105 is further away, but presumably the substitution of the bulky aliphatic valine for the more compact alanine results in a relaxation of the overall structure (see Figure 5). In general, these changes are expected to increase the flexibility around the chromophore and result in faster and more effective maturation of DsRed2. The other variants we analyzed were either slower in maturation or mature less completely than DsRed; we attribute this to the more limited free space around the chromophore in these variants. The variant DsRed_N42H is fast maturing²⁸ but shows a high green to red ratio which is inconsistent with the model. Clearly the substitution Asn42-His substitutes a smaller residue by a larger one, thus limiting the free space in the chromophore environment. This observation shows that flexibility is not the sole factor influencing maturation speed but that other mechanisms such as modified autocatalytic processes also speed up the maturation. In our analysis, we thus use only the final green to red intensity ratio and not the maturation speed to judge the flexibility of the chromophore environment. In our palette of proteins, the spectrally most different variant from DsRed is AG4, in which at two positions close to the chromophore smaller residues were substituted by larger ones (Val-71-Met and Ser-197-Thr), thereby distinctly restricting the free space around the chromophore and resulting in the almost exclusive formation of the GFP-like chromophore.

By considering the substitutions and the concept of Terskikh et al. which links the flexibility of the chromophore surrounding to the variants maturation and final spectral properties, the proteins analyzed here can be ordered by the flexibility around

the chromophore (starting with the variant with most flexibility) as follows:

DsRed2 – DsRed – Fluorescent Timer –
DsRed_N42H – AG4

This is the same sequence we found for the width of the distribution of single unit emission maximum positions starting with the narrowest distribution. Thus, analyzing the emission of the red form of the mature chromophore, we find for DsRed2 a distribution width $2\sigma = 5.0$ nm, for DsRed $2\sigma = 7.4$ nm, for Fluorescent Timer $2\sigma = 8.3$ nm, and for DsRed_N42H $2\sigma = 9.0$ nm. As the distribution of the photophysical parameters is strongly dependent on intrinsic parameters of the emitting chromophore (see above), the distributions of different chromophores in similar environments cannot directly be compared. However, the variant DsRed_N42H which shows distinct emission of both chromophores serves as a link between variants with the two different chromophores. For the GFP-like chromophore we find for DsRed_N42H $2\sigma = 7.0$ nm and for AG4 $2\sigma = 10.0$ nm.

Although the chemical surrounding of the chromophore was not systematically changed in the variants we analyzed, we paid attention to the fact that the variants have distinct differences in the chemical chromophore surroundings. Thus, in DsRed_N42H an imidazole ring, and in AG4 a sulfur group, was introduced into the chromophore vicinity, while in DsRed2 the polarity of the chromophore environment was altered by changing OH groups close to the chromophore. These alterations in the chemical environment of the chromophore do not disturb the trend between the flexibility of the chromophore environment and the distribution of emission maximum positions. For these proteins, the main factor determining the distribution is not the change in the chemical surrounding introduced by the mutations but the change in the packing of the chromophore in the protein. Interestingly a comparatively loose packing into the protein leads to a narrow distribution of emission maximum positions.

We speculate that the observed correlation between the width of the distribution of single unit emission maximum positions and the flexibility of the chromophore environment reflects the ability of the protein to return to the energetically most favorable conformation after, for example, a thermally induced reorientation. Flexible systems can easily return to their energetic minimum position by fast reorientation. In more rigid systems the return to the energetic minimum is reached in a more stepwise fashion, as certain energy barriers, here steric hindrances, need to be overcome. This principle applies to the ground state and to the excited state, as well as to reorientations of the chromophore environment during the excited-state lifetime. The embedded chromophore reports on conformations which are stable enough to be detected within the temporal resolution of the experiment, for example, manifested in different maxima positions,^{19,29} and thus resulting in a wider spread for more rigid systems. Spectral heterogeneity observed at the single molecule level is influenced by the structural heterogeneity of individual molecules. These observations may also be cast in terms of slower interconversion between individual protein conformers for those variants with more rigid nanoenvironments, thus leading to broader distributions.

(28) Bevis, B.; Glick, B. *Nat. Biotechnol.* **2002**, *20*, 83–87.

(29) Stracke, F.; Blum, C.; Becker, S.; Müllen, K.; Meixner, A. *Chem. Phys.* **2004**, *300*, 153–164.

Conclusions

We were able to demonstrate that with identical experimental settings and identical chromophore environments the spread of the distribution of emission maximum positions shows pronounced differences for different chromophores (see Figure 3d,e). Furthermore the spread of the emission maximum distribution is very sensitive to changes in the chromophore environment when the analyzed chromophore remains unchanged (see Figure 3a–d as well as Figure 3e, f). We were thus able to demonstrate that the spread of the emission maximum positions is a characteristic parameter of the respective chromophore–matrix system.

In addition we have been able to quantify the spread of the maximum distribution for DsRed and four of its variants and have been able to show that for different variants considerably different shifts between individual emitters have to be expected.

The observed differences in the distribution of the emission maximum positions are linked to differences in the conformational flexibility of the chromophores' nanoenvironment in the different variants. By using a concept first proposed by Terskikh and co-workers who showed that the chromophore maturation velocity and the green to red emitting chromophore ratio in DsRed variants depend on the flexibility around the chromophore, we were able to show that a flexible nanoenvironment of the chromophore results in a narrow distribution of the

emission maximum positions whereas a rigid nanoenvironment results in a broad distribution. Ordering the variants by the relative flexibility of the chromophore nanoenvironment using the previously reported concept yields the same sequence that we find using the width of distributions of the single unit emission maximum positions. This correspondence verifies the concept of Terskikh et al. Further changes of the chemical surrounding of the chromophore in the sampled variants did not disturb the correlation between the width of the distribution and the flexibility of the nanoenvironment of the chromophore, and thus these changes have only a minor effect on the observed distribution of emission maximum positions. We attribute the observed correlation between the rigidity of the chromophore environment and the distribution of emission maximum positions to the fact that more flexible systems can more easily return to their energetic minimum conformation.

Acknowledgment. Part of the experimental work reported in this paper was performed at the Physical Chemistry group at the University of Siegen, Germany. We thank the Deutsche Forschungsgemeinschaft for supporting this work with the Grant ME 1600/6-1. C. Blum's work at the University of Twente was supported by the MESA+ Institute for Nanotechnology.

JA060726G